THE JOURNAL OF PHYSICAL CHEMISTRY A

Article

pubs.acs.org/JPCA

Probing the Evaporation Dynamics of Ethanol/Gasoline Biofuel Blends Using Single Droplet Manipulation Techniques

Stella Corsetti,*[,†,‡] Rachael E. H. Miles,[¶] Craig McDonald,[‡] Yuri Belotti,[§] Jonathan P. Reid,[¶] Johannes Kiefer,[∥,†] and David McGloin[‡]

[†]School of Engineering, University of Aberdeen, Fraser Noble Building, Aberdeen AB24 3UE, Scotland, United Kingdom

[‡]SUPA, School of Science and Engineering, and [§]SUPA, Division of Physics, School of Engineering, Physics and Mathematics, University of Dundee, Nethergate, Dundee DD1 4HN, Scotland, United Kingdom

[¶]School of Chemistry, University of Bristol, Bristol, BS8 1TS, United Kingdom

[∥]Technische Thermodynamik, Universität Bremen, Badgasteiner Strasse 1, 28359 Bremen, Germany

ABSTRACT: Using blends of bioethanol and gasoline as automotive fuel leads to a net decrease in the production of harmful emission compared to the use of pure fossil fuel. However, fuel droplet evaporation dynamics change depending on the mixing ratio. Here we use single particle manipulation techniques to study the evaporation dynamics of ethanol/gasoline blend microdroplets. The use of an electrodynamic balance enables measurements of the evaporation of individual droplets in a controlled environment, while optical tweezers facilitate studies of the behavior of droplets inside a spray. Hence, the combination of both methods is perfectly suited to obtain a complete picture of the evaporation process. The influence of adding varied amounts of ethanol to gasoline is investigated, and we observe that droplets with a greater fraction of ethanol take longer to evaporate. Furthermore, we find that our methods are sensitive enough to observe the presence of trace amounts of water in the droplets. A theoretical model, predicting the evaporation of ethanol and gasoline droplets in dry nitrogen gas, is used to explain the experimental results. Also a theoretical estimation of the saturation of the environment, with other aerosols, in the tweezers is carried out.

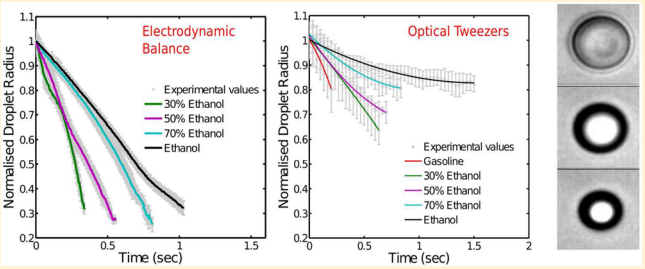

INTRODUCTION

The accumulation of greenhouse gases (GHG) in the atmosphere plays a significant role in global warming and climate change.[1] At present about 80% of the Earth's total energy supply is derived from the combustion of petroleum-based fossil fuel, which is the dominant source of carbon dioxide CO_2 and other GHG emissions.[2] Bioethanol, produced mainly from sugar cane, represents a potential green substitute to conventional fossil fuel.[3] The growing of sugar cane acts as a CO_2 sink reducing the net production of GHG.[4] The research into more efficient processes of ethanol production, based on the use of waste materials, such as waste paper, and biomass, is constantly advancing.[5,6] Today the use of pure ethanol as automotive fuel is mainly limited to Brazil. Blends of ethanol and gasoline are mostly used as fuels in Europe, U.S.A., Thailand, and Canada.[7] Mixing ratios up to 10% ethanol help in reducing CO_2 emissions without leading to any power reduction or spark-ignition engine modifications.[8] The stringent emissions regulations and limited oil resources pose questions around the possibility of using higher ethanol/gasoline blend ratios. However, the evaporation dynamics and thus the combustion process can be significantly affected by adding ethanol to gasoline.[9] The investigation of the evaporation of these blends at the single droplet level could give a more detailed picture of what happens during the atomization and combustion process and could help in avoiding extensive experimental testing. Single droplet studies make the experimental analysis of aerosol properties much more straightforward than those using complex many particle samples. In recent years, great effort has been made in developing accurate fuel and biofuel droplet evaporation models.[10−13] However, to confirm theoretical predictions, experimental observations are necessary.

Acoustic manipulation devices are suitable for studying large (~1 mm) droplets, but here we focus on tools readily capable of examining smaller droplets.[14] Electrodynamic balances (EDBs) and optical tweezers represent powerful tools to trap single aerosol droplets and enable their dynamics to be readily probed.[15] An EDB[16] uses electric fields to trap micron and submicron objects, while optical tweezers make use of focused light.[17] There are only a few experimental reports of the investigation of the evaporation of volatile droplets (containing components having a vapor pressure larger than 100 Pa) by either technique. Widmann and Davis used an EDB to

Received: October 15, 2015
Revised: December 2, 2015
Published: December 3, 2015

DOI: 10.1021/acs.jpca.5b10098
J. Phys. Chem. A 2015, 119, 12797−12804

investigate diesel fuel droplet evaporation.[18] However, there are no reports of the use of EDBs to probe the evaporation of ethanol/gasoline droplets. Optical tweezers have been largely used to observe and study physicochemical processes in real time, such as coagulation dynamics of airborne particles.[19] By using single and dual beam optical traps, evolving size, composition, temperature, and vapor pressure of semivolatile droplets have been investigated.[20] However, it is challenging to trap and investigate the evaporation of such volatile droplets as biofuels using tweezers.

MATERIALS AND METHODS

Biofuel Blends. A mixture of isooctane (2,2,4-trimethylpentane, Fisher Scientific, > 99%) and *n*-heptane (Fisher Scientific, >95%), with a ratio of 1:1 by weight, was used as a gasoline surrogate. Iso-octane and *n*-heptane are two primary reference fuels for gasoline, and they are used in many fundamental studies of engine combustion as a fuel surrogate.[21−25] Different ethanol−gasoline blends were prepared increasing stepwise the percentage in weight of ethanol (VWR, >99%).

Electrodynamic Balance (EDB). The EDB setup is shown in Figure 1. A voltage-activated dispenser (MicroFab MJ-APB-01) generates and ejects one droplet at a time (initial radius 25 μm) into a custom-made chamber. Droplets are trapped between two electrodes, in which a dc and an ac voltage are applied. The dc voltage is used to balance the Stoke's drag force exerted on the particle by a gas flow directed upward through the central cylindrical electrode, holding the particle in the center of the trap. The ac voltage compensates for the lateral displacements of the droplet.[26] Once a droplet is trapped, the angular profile of elastic light scattering from a 532 nm laser (Laser Quantum Ventus), operating at 10 mW, is recorded over a wide angular range using a Thorlabs CMOS camera (DCC1545M). The droplet's decreasing radius is estimated by analyzing the elastic light scattering collected, following the procedure described by Davies et al.[26] Droplet size information is collected every 0.005 s.

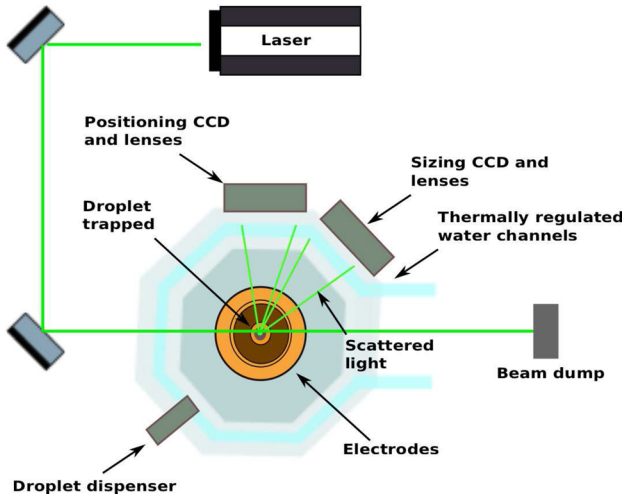

Figure 1. Electrodynamic balance (EDB) setup.

Measurements were carried out at 280 K and ambient pressure. Nitrogen was directed through the outer cylindrical electrode (flow rate of 50 sccm, resulting in a velocity of around 1 cm s^{-1} over the droplet) to establish a controlled environment (<5% RH). The temperature within the EDB was controlled by pumping a 50:50 (w/w) water/ethylene glycol solution through the base and lid portions of the trapping cell using a recirculating water bath (Julabo F-32). The water bath had a working temperature range 238−473 K but was limited to a maximum of 280 K in this study by the minimum droplet evaporation rate that could be determined by light scattering. To record droplet evaporation profiles over 1 s or longer, it was necessary to cool the droplet and gas flow to a temperature of 280 K; otherwise, the droplet vapor pressure is so high that evaporation occurs faster than can be probed. The nitrogen gas flow passed through the base portion of the trapping cell as it entered the EDB, thereby equilibrating to the same temperature as the circulating coolant. The temperature in the center of the trap was measured directly using a probe (Tenma 72-2060) with stability better than 0.1 K, and it was this value that was used in subsequent theoretical modeling calculations. Furthermore, it was not possible to trap uncharged droplets (such as pure gasoline) and challenging to trap droplets with small charge (low ethanol content).

Optical Tweezers. The trapping laser, a 532 nm laser (Laser Quantum Finesse), with maximum output of 5 W, is expanded to slightly overfill the back aperture of a 100× infinity corrected oil immersion microscope objective (Nikon E plan, NA = 1.25). Aerosols of the blends prepared are generated by using an Aerosonic nebulizer (initial radius of droplets ranging from 6.4 to 8 μm) and passed into a custom-made chamber positioned on a glass coverslip (aerosols flow rate of ≃0.7 mL/min). The laser is focused slightly above the cover slip and above any aqueous layer formed by falling aerosols. The cover slip is treated by a hydrophilic substance (Decon 90) to avoid aerosols falling onto the slide and acting as lenses. The power in the trap was ≃5 mW. Aerosols are imaged by using an AVT Guppy CCD camera (30 fps). Figure 2 shows the optical tweezers setup used.

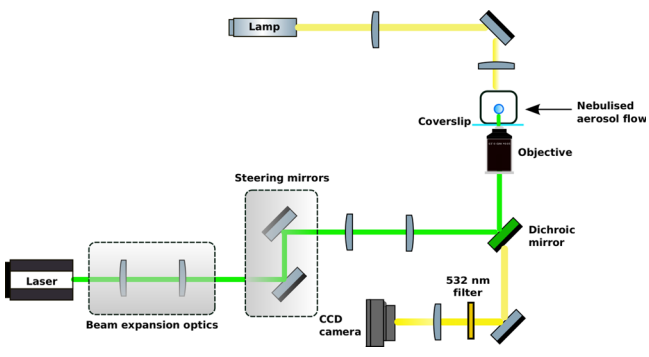

Figure 2. Diagram of the optical tweezers setup.

Measurements were taken at 293 K, ambient pressure, and ambient humidity (≃50% RH). A single ethanol/gasoline droplet was captured from a flow of other aerosols. In the tweezers all the droplets were trapped in an initial condition of saturation of the environment with the mixtures' vapor. In such ambient conditions, the vapor pressure difference between the droplet surface and that at infinite distance is zero.

It was not readily possible to trap a droplet in a dry, low humidity environment using the tweezers, because of the low propability to trap, compared to the EDB. However, droplets do not need to be charged to be trapped in the tweezers, so, unlike the EDB, it was possible to trap pure gasoline and

DOI: 10.1021/acs.jpca.5b10098
J. Phys. Chem. A 2015, 119, 12797−12804

droplets with low ethanol content. Also, because of the saturation of the environment, it was possible to trap droplets at a temperature above 280 K. In the optical tweezers measurements, the change in the droplet radius was estimated by video analysis using a custom-made Matlab program. During evaporation, each droplet was well trapped with its external contour visible until it became too small to be trapped and escaped. The image of a trapped ethanol/gasoline droplet at three different frames is shown in Figure 3. ImageJ was used to

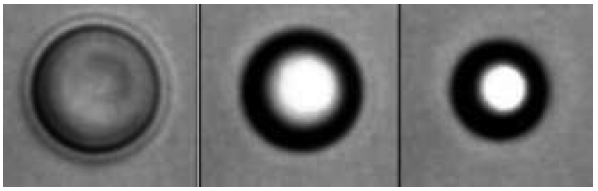

Figure 3. Evolution in size of an optically trapped aerosol droplet. Image at $t = 0$, $t = 0.23$, and $t = 0.5$ s. Each square around the droplets represents 20 μm in size.

extract kymographs (plots of spatial changes with respect to time) of the diameter from each evaporating droplet. A Matlab Graphical User Interface (GUI) has been developed with the aim of quantitatively analyzing the kymographs. It uses an algorithm able to detect the edge of the droplet based on the intensity difference (Figure 4). The algorithm calculates the

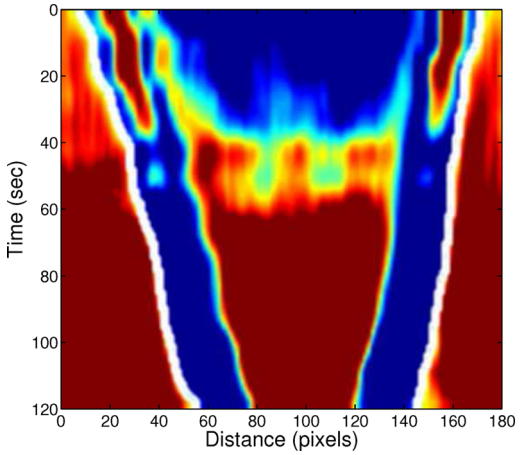

Figure 4. Kymograph of the diameter of an evaporating droplet. The white line indicates the edge of the droplet.

spatial distance between the two previously detected edges at each time step. The temporal evolution of the droplet radius in micrometers is calculated by knowing how the pixel size relates to the physical size. In our system one pixel equates to 0.09 μm. Some of the videos were analyzed by fitting a circle around the droplet and evaluating the circumference (at each time step) from which the radius was estimated. This procedure was mostly used for videos in which the evaporation of droplets occurred so fast that the kymographs were not clear. For each fuel blend, five droplets were trapped and analyzed using the protocol described above.

The time at which each droplet was trapped and its contour became visible was taken as the initial time ($t = 0$). The time series stops when the droplet escaped from the trap or it is no longer well visible.

RESULTS

Experimental Evaporation Trends. The evaporation trends of different mass ratio ethanol/gasoline droplets, trapped by the EDB and the tweezers, are shown in Figure 5. The

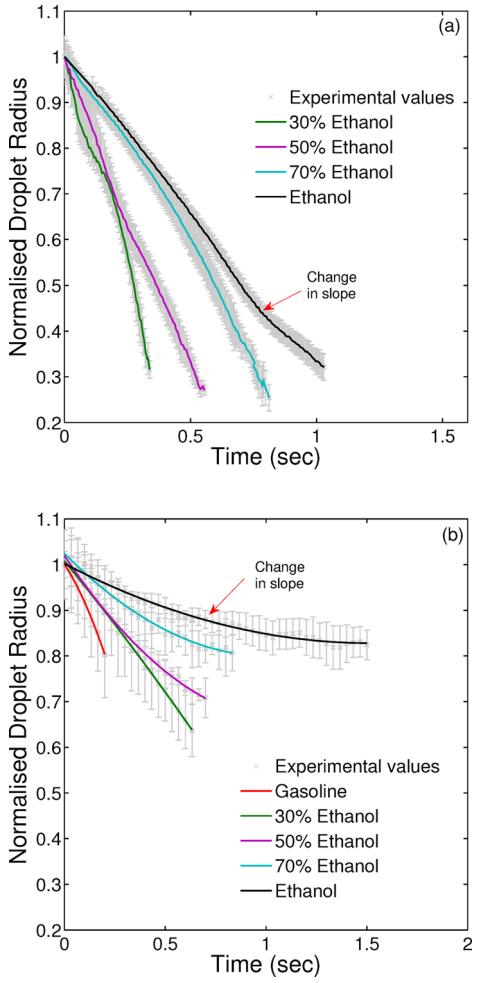

Figure 5. Evaporation trends of ethanol/gasoline droplets trapped by EDB (a) and tweezers (b). The radius of the droplet, normalized with respect to the initial droplet size versus time, is shown. The error bars represent the standard deviation in the radius associated with each time-resolved size. In (a) full lines represent joining of experimental data points. Radius estimated at a time resolution of 0.006 s. In (b) full lines represent fitting of experimental data. Radius estimated at a time resolution of 0.033 s.

droplet radius, normalized with respect to the initial size of the droplet, is plotted versus time. In the EDB measurements the initial size of the droplets in the figure corresponds to the size at which they entered the trap and the sizing algorithm was first able to determine a size. There is a time period of typically around 0.1 s between a particle being generated and it entering the trap during which no sizing data can be recorded, and so this portion of the evaporation has been neglected. In the tweezers the initial size of the droplets corresponds to the size at which droplets enter the trap and their contour became clear (maximum delay about 0.2 s). In the EDB and tweezers measurements, each evaporation curve represents the mean of the observations from 10 and 5 droplets, respectively. Droplets containing a higher percentage of ethanol resulted in longer lifetimes in both experiments. The trends confirm the results

DOI: 10.1021/acs.jpca.5b10098
J. Phys. Chem. A 2015, 119, 12797−12804

we obtained by analyzing ethanol/gasoline blends, at the molecuar level, in a previous work.[27] It is evident that in the tweezers experiment the droplets take longer to evaporate compared to the droplets trapped in the EDB, even though they are at higher ambient temperature. Also, the evaporation of pure ethanol in each experiment shows two different slopes (the location point of the change in slope is indicated in Figure 5). According to the study performed by Saharin et al.,[28] the first slope represents the evaporation of pure ethanol, and the second one represents ethanol evaporation, but from a droplet that has a large amount of water in it, suppressing the mole fraction of ethanol and thus the mass flux of ethanol from the droplet. Ethanol, being miscible to water, absorbs ambient water vapor.[29] Saharin[30] also demonstrated that the ambient relative humidity affects the value of final vaporization rate, which is observed to decrease as the ambient relative humidity increases. The change in slope is not obvious in the ethanol evaporation curve obtained with the tweezers, so the evaporation trend of ethanol droplets trapped by the tweezers has been plotted again, with a different y scale and indicating the point in which the change in the slope occurs, in Figure 6.

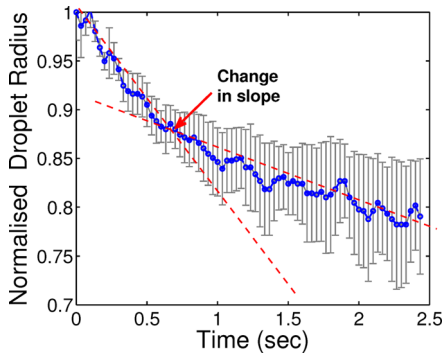

Figure 6. Evaporation trends of ethanol droplets trapped by the optical tweezers. The radius of the droplet, normalized with respect to the initial droplet size versus time, is shown. In blue, the experimental data. The red dashed lines represent a linear trend of the two different slopes. The point in which the change in the slope occurs is indicated.

The high RH in the tweezers experiments, together with a saturation of the environment (affecting the first slope of the evaporation), could be the reason for the longer evaporation time of the pure ethanol droplets with respect to the EDB experiments. In the EDB, droplets are trapped in a chamber filled with nitrogen gas, which should exclude the effect of ambient humidity on the evaporation process. However, there is still some humidity in the chamber, which is in contact with the external environment through the inlet point of the aerosols. This could explain why in the EDB experiments the ethanol evaporation curve also presents two slopes.

Considering the higher vapor pressure of pure ethanol with respect to the gasoline surrogate at 280 K (Table 1), droplets with a higher percentage of ethanol should evaporate faster.

Theoretical Model. With the aim of understanding why ethanol evaporates more slowly than gasoline, a theoretical model was used to predict the evaporation trends of pure ethanol and pure *n*-heptane and isooctane droplets, in the more simple environmental conditions of nitrogen around the droplet. The parameters used in the model for the different components are detailed in Table 1.

Table 1. Thermophysical Properties of Ethanol, Gasoline, and Nitrogen Calculated at 280 K

properties	ethanol	*n*-heptane	isooctane	nitrogen
molecular weight (kg/mol)	0.046	0.1	0.114	0.028
density liquid (kg/m^3)	801	695	698.7	
dynamic viscosity (Pa/s)				16.98×10^{-6}
binary diffusion coefficient (cm^2/s)	1.1×10^{-5}	6.58×10^{-6}	6.7×10^{-6}	
thermal conductivity (W/m K)				0.024
specific heat capacity (J/kg K)	2550	2180	2037	
latent heat (J/kg)	1.04×10^6	3.72×10^5	3.07×10^5	
A	8.32109	6.905113	6.820137	
B	1718.10	1269.821	1262.707	
C	237.52	217.110	221.307	
vapor pressure (Pa)	2627.7	2291.7	2574.3	

The temporal evolution of the droplet surface temperature T_s can be expressed through the change of energy of the droplet surface. This energy is the sum of conductive heat transfer and the heat of vaporization and is given by[31]

$$m_p c_l \frac{dT_s}{dt} = 4\pi R_p^2 w(T_g - T_s) + \dot{m}_p L \quad (1)$$

where m_p is the droplet mass, c_l the specific heat, R_p the radius of the droplet, w the thermal conductivity of the gas phase, and L the latent heat of vaporization. $\dot{m}_p$ is the rate of change of the droplet mass, and for a single component droplet evaporating in nitrogen was described by Spalding as[32]

$$\dot{m}_p = \frac{dm_p}{dt} = -2\pi R_p Sh \rho_g D_f \ln(1 + B_m) \quad (2)$$

where D_f and ρ_g are the binary diffusion coefficient and the density of the gaseous phase, respectively. Sh is the Sherwood number, which represents the ratio of convective to diffusive mass transport. It is expressed by[33]

$$Sh = 2 + 0.552 Re^{1/2} Sc^{1/3} \quad (3)$$

Re and Sc are the Reynolds and Schmidt numbers, evaluated in the gaseous phase. They are given by

$$Re = \frac{\rho_g d_p v}{\eta_g} \quad (4)$$

$$Sc = \frac{\eta_g}{\rho_g d_p} \quad (5)$$

v is velocity of the droplet relative to the surrounding gas, which is equal to the velocity of nitrogen gas over the droplet. η_g is the nitrogen dynamic viscosity. B_m is the Spalding mass number, which has the following expression[32]

$$B_m = \frac{Y_s - Y_\infty}{1 - Y_s} \quad (6)$$

Y_s and Y_∞ are the mass fractions of ethanol (or gasoline components) vapor near the droplet surface and in the ambient gas, respectively. Y_∞ can be neglected and considered equal to zero in the EDB measurements. The mass fraction of the

DOI: 10.1021/acs.jpca.5b10098
J. Phys. Chem. A 2015, 119, 12797−12804

component near the droplet surface can be evaluated from the mole fraction x_s, which is given by

$$x_s = \frac{p_{vap}}{p_{amb}} \tag{7}$$

p_{vap} is the vapor pressure of ethanol (or the gasoline components) and p_{amb} is the ambient air pressure, both in Pascal. p_{vap} of ethanol has been calculated using the Antoine equation

$$p_{vap} = c10^{(A-B/C+(T-273.15))} \tag{8}$$

c = 133.322 is a constant used to convert mmHg to Pa, T is the droplet surface temperature, in K, and A, B, and C are component specific constants (values in Table 1). The vapor pressure of pure ethanol has been calculated using the constants reported by Dean,[34] while for pure n-heptane and isooctane the constants reported by Smith[35] have been used. Finally, the mass fraction of ethanol (or gasoline components) near the droplet surface can be expressed as

$$Y_s = \frac{x_s M_{e,g}}{x_s M_{e,g} + (1 - x_s) M_n} \tag{9}$$

$M_{e,g}$ and M_n are the molecular weights of ethanol (or gasoline components) and nitrogen, respectively.

Theoretical Evaporation of Single Ethanol and Gasoline Droplets. A prediction of the surface temperature of evaporating pure ethanol, pure n-heptane, and pure isooctane droplets has been carried out using the thermophysical properties shown in Table 1. The initial ethanol droplet's radius was set equal to the initial size determined for ethanol droplets trapped in the EDB (23.6 μm). The initial n-heptane and isooctane droplet's radius was set equal to the initial size determined for 50%/50% w/w ethanol and n-heptane and 50%/50% w/w ethanol and isooctane droplets trapped in the EDB (21.3 and 21.7 μm, respectively). The ambient conditions were set equal to the ones in the EDB experiment (T_{amb} = 280 K and ambient pressure).

As the evaporation starts, the droplet surface temperature decreases rapidly, approaching the value at which the rate of heat loss from the droplet by evaporation is balanced by the rate of heat transferred to the droplet from the surrounding gas phase (wet bulb temperature). This results in ethanol droplets reaching a lower temperature (269 K) than the gasoline ones (273.58 and 273.22 K for n-heptane and isooctane, respectively). The lower temperature of evaporating ethanol droplets comes from the larger latent heat of ethanol than the hydrocarbons in the gasoline mix (see Table 1). This has an effect on the vapor pressure of the components (vapor pressure of ethanol, n-heptane, and isooctane at their wet bulb temperatures are calculated to be 1213, 1559.6, and 1742.5 Pa respectively), which drives the net mass flux, and therefore the droplet lifetime. This is the cause of the slower evaporation of ethanol droplets. However, neither the EDB or tweezers measurements have sufficient time resolution to probe the very early time unsteady evaporation during which droplet cooling occurs.

This behavior also affects the mixtures and explains the trends observed in Figure 5. Droplets with a higher percentage of ethanol will experience a lower surface temperature and therefore a slower evaporation. In addition, the evolution of the radius of a pure ethanol, n-heptane, and isooctane droplet was calculated. The same intial radii to calculate the droplets surface temperature were used. Figure 7 shows the theoretical

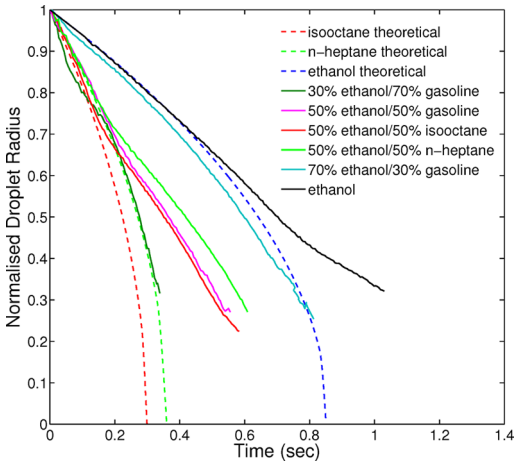

Figure 7. Evaporation curves: dashed lines are for droplets of pure isooctane, n-heptane, and ethanol. Solid lines are the experimental evaporation of different ratios of ethanol/gasoline droplets.

evaporation of the pure components droplets and the experimental evaporation of different mass ratio ethanol/gasoline droplets. The theoretical evaporation of isooctane and n-heptane droplets is very similar due to the similar characteristic of the components (see Table 1). This is supported by the similar experimental trends in evaporation of 50%/50% w/w ethanol and n-heptane and 50%/50% w/w ethanol and isooctane droplets, with the droplet containing isooctane evaporating slightly faster than that containing n-heptane. The evaporation trends of different ratio ethanol/gasoline droplets fall within the limits of the theoretical evaporation of the pure components. Finally, in Figure 8 the

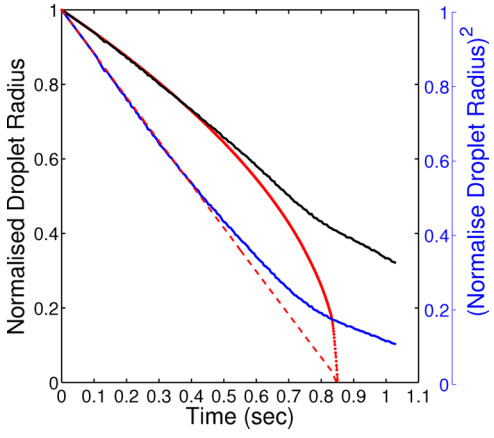

Figure 8. Comparison between theoretical and experimental results for ethanol droplet evaporation time. In red, the model. The blue and black lines represent respectively the normalized decreasing size and the evaporation rate.

theoretical evaporation of ethanol droplets is compared with the experimental values. The model diverges significantly from the experimental evaporation of ethanol at longer time scales. We suggest that the reason for this is a retardation of the ethanol evaporation due to water uptake from the ambient. At the present the model does not take into account the impact of water uptake into the fuel droplets, and further investigation is

DOI: 10.1021/acs.jpca.5b10098
J. Phys. Chem. A 2015, 119, 12797−12804

necessary to include these details. However, the model was found to predict quite well the first part of the evaporation of pure ethanol droplets (with no water content) trapped in the EBD.

Calculation of the Saturation of the Environment in the Tweezers. If the gas far from the evaporating droplet is not free of the diffusing vapor, as in the case of the tweezers experiments, according to Maxwell, the change of droplet mass can be written as[18]

$$\frac{dm}{dt} = -\frac{4\pi R_p D_f M_e}{R}\left[\frac{P^0(T_s)}{T_s} - \frac{P_\infty}{T_\infty}\right] \quad (10)$$

in which R is the gas constant, P^0 is the vapor pressure of ethanol near the droplet surface calculated at the droplet surface temperature T_s, and P_∞ and T_∞ are the partial pressure and the temperature of the ethanol vapor in the bulk gas, respectively. The others symbols retain the same meaning as before. Equation 10 can be written also in terms of squared droplet radius

$$\frac{dR_p^2}{dt} = -\frac{2D_f M_e}{\rho_l R}\left[\frac{P^0(T_s)}{T_s} - \frac{P_\infty}{T_\infty}\right] \quad (11)$$

Integrating eq 11 over the droplet radius and time the following expression for the squared droplet's radius is found:

$$R_p^2 = -\left(\frac{2D_f M_e}{\rho_l R}\left[\frac{P^0(T_s)}{T_s} - \frac{P_\infty}{T_\infty}\right]\right)t + R_0^2 \quad (12)$$

From eq 12 the slope of the curve radius squared versus time, and then the evaporation constant, S, is given by

$$S = -\frac{2D_f M_e}{\rho_l R}\left[\frac{P^0(T_s)}{T_s} - \frac{P_\infty}{T_\infty}\right] \quad (13)$$

In order to get information about the composition of the gas phase in the optical tweezers experiments, during the evaporation of a pure ethanol droplet, eq 13 was used to calculate the vapor pressure of ethanol in the ambient (P_∞). The evaporation constant, S, for the ethanol droplets evaporating in the tweezers was found to be equal to 1.6×10^{-11} m^2/s (see Figure 9).

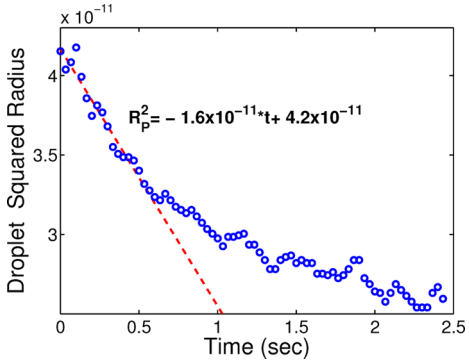

Figure 9. Determination of the slope of the curve radius squared versus time, representing the evaporation constant, for ethanol droplets evaporating in the tweezers. In blue, the experimental data. In red is the linear fitting of the pure ethanol evaporation part of the curve.

Equation 1 was used to calculate the surface temperature, T_s, of a pure ethanol droplet having an initial radius equal to the one determined for ethanol droplets trapped in the tweezers (6.44 μm), at T_{amb} = 293 K. The parameters used to calculate T_s are summarized in in Table 2. The vapor pressure of ethanol near the droplet's surface was then calculated by using eq 8. The values of T_s, $P^0(T_s)$, and P_∞ are summarized in Table 3.

Table 2. Thermophysical Properties of Ethanol, *n*-Heptane, and Isooctane at 293 K

properties	ethanol	*n*-hepatne	isooctane	nitrogen
molecular weight (kg/mol)	0.046	0.1	0.11	0.028
density liquid (kg/m^3)	789	679	688	
dynamic viscosity (Pa/s)				17.58×10^{-6}
binary diffusion coefficient (cm^2/s)	1.27×10^{-5}	6.95×10^{-6}	6.97×10^{-6}	
thermal conductivity (W/m K)				0.025

Table 3. Parameters Calculated To Determine the Ambient Saturation in the Tweezers

properties	ethanol	*n*-hepatne	isooctane
T_s (K)	275	282.16	282.32
$P^0(T_s)$ (Pa)	1855	2554	2896
P_∞ (Pa)	1983	2488	2731
$P(T_{amb} = 293\ K)$ (Pa)	5893.7	4690	5116

The vapor pressure of ethanol in the ambient is similar to the vapor pressure of ethanol near the droplet's surface, suggesting that the particle is almost in equilibrium with the gas phase, which is why the size changes are much smaller and slower than the ones observed in the EDB (where P_∞ was zero). To determine how close P_∞ is to ethanol saturation, the equilibrium vapor pressure of the component at ambient temperature, $P(T_{amb} = 293\ K)$, was calculated (value reported in Table 3) and compared to (P_∞). Saturation is approached when P_∞ is close to $P(T_{amb})$. We find that the ratio between P_∞ and the equilibrium vapor pressure is 0.33 suggesting that the environment could be saturated with ~33% of ethanol vapor.

We also estimated the saturation of the environment in the tweezers in the case of gasoline droplets evaporation, following the same procedure as for the ethanol droplets. The evaporation constant, S, for the gasoline droplets was found to be equal to 6.9×10^{-11} m^2/s. The surface temperatures of a pure *n*-heptane droplet and a pure isooctane droplet, having an initial size equal to the one determined in the tweezers experiments for gasoline droplets (6.26 μm), at 293 K, were calculated using the values reported in Table 2. The value of T_s, $P^0(T_s)$, and P_∞ and $P(T_{amb})$ are reported in Table 3. Whether the gasoline droplet is approximated as a pure *n*-heptane droplet or a pure isooctane droplet, the value of P_∞ is very similar to the value of P^0, suggesting that the gasoline particle is almost in equilibrium with the gas phase. The ratio between P_∞ and $P(T_{amb})$ was found to be equal to 0.53 in both cases in which the gasoline droplet was considered as pure *n*-heptane and as pure isooctane. This suggests that in the case of the gasoline droplets evaporating in the tweezers, the environment could be saturated with ~ 50% of *n*-heptane/isooctane vapor.

DOI: 10.1021/acs.jpca.5b10098
J. Phys. Chem. A 2015, 119, 12797−12804

CONCLUSIONS

In this work preliminary measurements of the evaporation of ethanol/gasoline blends, with different ethanol content, at the single droplet level have been carried out. Two different techniques, EDB and optical tweezers, have been used to trap the droplets. An EDB has been used to trap droplets in nitrogen, while optical tweezers have been used to trap them in a flow of other ethanol/gasoline aerosols: a more complex environment. In both environments droplets with a higher percentage of ethanol resulted in longer lifetimes. A theoretical model has been used to predict the evaporation rates of pure ethanol and pure gasoline droplets in nitrogen. The slower evaporation of the ethanol droplets with respect to the gasoline droplets has been related to a bigger decrease in the droplets surface temperature during the evaporation. A more complete model predicting the evaporation rates of different ratio ethanol/gasoline droplets will be developed in the future. Furthermore, a theoretical estimation of the saturation of the environment, with other aerosols, in the tweezers has been given. In outlining the differences between the two techniques, we emphasize that the impossibility of trapping uncharged droplets (such as pure gasoline) and the fast evaporating components at high temperature by using the EDB suggests that techniques such as optical tweezers are important for such studies. The ability of tweezers to easily trap from a spray is also an advantage, as is the ability of tweezers to be integrated into, for example, optical fibers,[36] which will allow trapping within more hostile environments, such as engines. Better control of the environment in the optical tweezers chamber would open up the potential to perform more quantitative analysis in complex environmental conditions. Our techniques suggest that optical tweezers are a very useful tool for studying binary and higher order volatile droplets and enable very precise evaporation dynamics to be followed, with the ability to measure the dynamics of different droplet components. In the case of the study of biofuels, it is hoped that by combining with techniques to measure at high and controlled pressures[37] our system can explore environments more directly linked to engines, opening up the possibility of studying combustion processes with these tools.[38]

AUTHOR INFORMATION

Corresponding Author

*E-mail: s.corsetti@dundee.ac.uk.

Notes

The authors declare no competing financial interest.

ACKNOWLEDGMENTS

This work was supported by the Northern Research Partnership (NRP) and the Engineering and Physical Sciences Research Council (EPSRC), grant EP/G007713/1.

REFERENCES

(1) Ramanathan, V.; Crutzen, P. J.; Kiehl, J. T.; Rosenfeld, D. Aerosols, climate, and the hydrological cycle. *Science (Washington, DC, U. S.)* **2001**, *294*, 2119−2124.

(2) International Energy Agency. CO_2 Emissions from Fuel Combustion Highlights, 2013.

(3) Balat, M.; Balat, H. Recent trends in global production and utilization of bio-ethanol fuel. *Appl. Energy* **2009**, *86*, 2273−2282.

(4) De Oliveira, M. E. D.; Vaughan, B. E.; Rykiel, E. J. Ethanol as fuels: Energy, carbon dioxide balances, and ecological footprint. *BioScience* **2005**, *55*, 593−602.

(5) Wang, L.; Sharifzadeh, M.; Templer, R.; Murphy, R. J. Technology performance and economic feasibility of bioethanol production from various waste papers. *Energy Environ. Sci.* **2012**, *5*, 5717−5730.

(6) Caspeta, L.; Buijs, N. A.; Nielsen, J. The role of biofuels in the future energy supply. *Energy Environ. Sci.* **2013**, *6*, 1077−1082.

(7) Carriquiry, M. A.; Du, X.; Timilsina, G. R. Second generation biofuels: Economics and policies. *Energy Policy* **2011**, *39*, 4222−4234.

(8) Masum, B.; Masjuki, H.; Kalam, M.; Rizwanul Fattah, I.; Palash, S.; Abedin, M. Effect of ethanol−gasoline blend on NOx emission in SI engine. *Renewable Sustainable Energy Rev.* **2013**, *24*, 209−222.

(9) Turner, D.; Xu, H.; Cracknell, R. F.; Natarajan, V.; Chen, X. Combustion performance of bio-ethanol at various blend ratios in a gasoline direct injection engine. *Fuel* **2011**, *90*, 1999−2006.

(10) Barata, J. Modelling of biofuel droplets dispersion and evaporation. *Renewable Energy* **2008**, *33*, 769−779.

(11) Hallett, W. L. H.; Beauchamp-Kiss, S. Evaporation of single droplets of ethanol−fuel oil mixtures. *Fuel* **2010**, *89*, 2496−2504.

(12) Zhang, L.; Kong, S. C. Multicomponent vaporization modeling of bio-oil and its mixtures with other fuels. *Fuel* **2012**, *95*, 471−480.

(13) Sazhin, S. S.; Al Qubeissi, M.; Kolodnytska, R.; Elwardany, A. E.; Nasiri, R.; Heikal, M. R. Modelling of biodiesel fuel droplet heating and evaporation. *Fuel* **2014**, *115*, 559−572.

(14) Saha, A.; Kumar, R.; Basu, S. Infrared thermography and numerical study of vaporization characteristics of pure and blended bio-fuel droplets. *Int. J. Heat Mass Transfer* **2010**, *53*, 3862−3873.

(15) Krieger, U. K.; Marcolli, C.; Reid, J. P. Exploring the complexity of aerosol particle properties and processes using single particle techniques. *Chem. Soc. Rev.* **2012**, *41*, 6631−6662.

(16) Davis, E. J.; Ray, A. Single aerosol particle size and mass measurements using an electrodynamic balance. *J. Colloid Interface Sci.* **1980**, *75*, 566−576.

(17) Ashkin, A.; Dziedzic, J.; Bjorkholm, J.; Chu, S. Observation of a single-beam gradient force optical trap for dielectric particles. *Opt. Lett.* **1986**, *11*, 288−290.

(18) Widmann, J.; Davis, E. Evaporation of multicomponent droplets. *Aerosol Sci. Technol.* **1997**, *27*, 243−254.

(19) McGloin, D. Optical tweezers: 20 years on. *Philos. Trans. R. Soc., A* **2006**, *364*, 3521−3537.

(20) Cai, C.; Stewart, D. J.; Reid, J. P.; Zhang, Y.-h.; Ohm, P.; Dutcher, C. S.; Clegg, S. L. Organic Component Vapor Pressures and Hygroscopicities of Aqueous Aerosol Measured by Optical Tweezers. *J. Phys. Chem. A* **2015**, *119*, 704−718. PMID: 25522920.

(21) Mehl, M.; Pitz, W. J.; Westbrook, C. K.; Curran, H. J. Kinetic modeling of gasoline surrogate components and mixtures under engine conditions. *Proc. Combust. Inst.* **2011**, *33*, 193−200.

(22) Feng, H.; Zhang, C.; Wang, M.; Liu, D.; Yang, X.; Lee, C.-f. Availability analysis of *n*-heptane/iso-octane blends during low-temperature engine combustion using a single-zone combustion model. *Energy Convers. Manage.* **2014**, *84*, 613−622.

(23) Banerjee, R. Numerical investigation of evaporation of a single ethanol/iso-octane droplet. *Fuel* **2013**, *107*, 724−739.

(24) Keller, P.; Bader, A.; Hasse, C. The influence of intra-droplet heat and mass transfer limitations in evaporation of binary hydrocarbon mixtures. *Int. J. Heat Mass Transfer* **2013**, *67*, 1191−1207.

(25) Curran, H. J.; Pitz, W.; Westbrook, C.; Callahan, G.; Dryer, F. Oxidation of automotive primary reference fuels at elevated pressures. *Symp. Combust., [Proc.]* **1998**, *27*, 379−387.

(26) Davies, J. F.; Haddrell, A. E.; Reid, J. P. Time-resolved measurements of the evaporation of volatile components from single aerosol droplets. *Aerosol Sci. Technol.* **2012**, *46*, 666−677.

(27) Corsetti, S.; Zehentbauer, F. M.; McGloin, D.; Kiefer, J. Characterization of gasoline/ethanol blends by infrared and excess infrared spectroscopy. *Fuel* **2015**, *141*, 136−142.

(28) Saharin, S.; Lefort, B.; Morin, C.; Chauveau, C.; le Moyne, L.; Kafafy, R. Vaporization characteristics of ethanol droplets: Influence of the environment humidity. ASME 2011 Turbo Expo: Turbine Technical Conference and Exposition, 2011; pp 669−676.

DOI: 10.1021/acs.jpca.5b10098
J. Phys. Chem. A 2015, 119, 12797−12804

(29) Lee, A.; Law, C. An experimental investigation on the vaporization and combustion of methanol and ethanol droplets. *Combust. Sci. Technol.* **1992**, *86*, 253−265.
(30) Binti Saharin, S. Vaporization and autoignition characteristics of ethanol and 1-propanol droplets: Influence of water. Ph.D. Thesis, Dijon, 2013.
(31) CroweC.*Conservation equations for vapor-droplet flows including boundary-droplet effects*; Lawrence Livermore Laboratory, University of California: Livermore, CA, 1976
(32) Spalding, D. B. The combustion of liquid fuels. *Symp. Combust., [Proc.]* **1953**, *4*, 847−864.
(33) Ranz, W. E.; Marshall, W. R. Evaporation from drops. *Chem. Eng. Prog.* **1952**, *48*, 141−146.
(34) Dean, J. A. *Lange's Handbook of Chemistry*; McGraw Hill Book Co.: New York, 1985.
(35) Smith, E. R. Boiling points of *n*-heptane and 2,2.4-trimethyl pentane over the range 100 to 1'soo-millimiter pressure. *J. Res.Natl. Bur. Stand.* **1940**, *24*, 229.
(36) Gong, Y.; Ye, A.-Y.; Wu, Y.; Rao, Y.-J.; Yao, Y.; Xiao, S. Graded-index fiber tip optical tweezers: Numerical simulation and trapping experiment. *Opt. Express* **2013**, *21*, 16181−16190.
(37) Bowman, R. W.; Gibson, G. M.; Padgett, M. J.; Saglimbeni, F.; Di Leonardo, R. Optical trapping at gigapascal pressures. *Phys. Rev. Lett.* **2013**, *110*, 095902.
(38) Li, S.-J.; Huang, X.-F. The manipulation and combustion of carbon-based micro particles by optical tweezers. *Int. J. Optomechatronics.* **2015**, *9*, 35−47.

DOI: 10.1021/acs.jpca.5b10098
J. Phys. Chem. A 2015, 119, 12797−12804